Cancer Chemother Pharmacol (1998) 42: 300–306

ORIGINAL ARTICLE

Joel E. Wright · Maria Pardo · Anatoly Tretyakov
Wendy L. Alperin · Dorothy Trites · Andre Rosowsky

Pharmacokinetics, antifolate activity and tissue distribution of PT523 in SCC VII tumor-bearing mice

Received: 8 August 1997 / Accepted: 12 November 1997

Abstract *Purpose*: To monitor the pharmacokinetics of PT523 and methotrexate in C3H mice with transplanted SCC VII tumors; to compare the impact of PT523 and methotrexate on tumor and normal host 5,10-methylenetetrahydrofolate levels; and to synthesize [^{14}C]PT523 and determine its time-dependent tissue distribution in tumor and host tissues. *Methods*: C3H mice bearing SCC VII tumors were given i.p. PT523 or methotrexate. Plasma drug levels and tumor, gut and marrow 5,10-methylenetetrahydrofolate were assayed. [^{14}C]PT523 was synthesized and administered i.v. to tumor-bearing mice for tissue distribution analysis. *Results*: Areas under the curve, mean residence times, whole body clearances, apparent distribution volumes, and plasma protein binding of PT523 vs methotrexate were, respectively, 4311 vs 6472 $\mu M \cdot min^{-1}$; 20 vs 16 min; 0.56 vs 0.36 $ml \cdot min^{-1}$; 532 vs 325 $ml \cdot kg^{-1}$; and 70% vs 30%. Both PT523 and methotrexate caused time-dependent declines in 5,10-methylenetetrahydrofolate in tumor and gut mucosa, but not in marrow. Gut levels began to recover within 4 h in the PT523-treated group only. [^{14}C]PT523 distributed mainly into the liver, duodenum, kidneys, lungs, tumor, pancreas and muscle; less into the spleen, blood cells, heart, brain and testicles; and very little into bone marrow. Only 35% of the dose was excreted, and 2.9-fold more in feces than urine. *Conclusions*: Despite its more rapid clearance, accumulation of PT523 in extravascular tissues was greater than that of methotrexate. Consequently, less PT523 was recovered in feces and urine and its apparent volume of distribution was greater. PT523 selectively depleted 5,10-methylenetetrahydrofolate pools in tumor and, less persistently, in gut mucosa, but spared the marrow. [^{14}C]PT523 tissue distribution correlated with organ mass and blood supply.

Key words Pharmacokinetics · Tissue distribution · Nonpolyglutamatable antifolate · Murine tumor model

This work was supported by Grants RO1-CA19589 and CA25394 from the National Cancer Institute

J.E. Wright (✉) · M. Pardo · A. Tretyakov · W. L. Alperin · D. Trites[1] · A. Rosowsky
Dana-Farber Cancer Institute,
44 Binney Street, Boston, MA 02115, USA
Tel. +1-617-632-3123; Fax +1-617-632-2410

J.E. Wright · A. Rosowsky
Department of Biological Chemistry and Molecular Pharmacology, Harvard Medical School, Boston, MA, USA

[1] Deceased

Introduction

A number of studies have shown that resistance to the classical antifolate, methotrexate (MTX), may result from its inadequate polyglutamylation within certain tumors [14–16]. Such tumors have low folyl polyglutamate synthetase (FPGS) [1, 2, 4, 18, 28, 40] or high folyl polyglutamate hydrolase (FPGH) activity [25]. Among the three newer agents now in clinical trials that specifically target dihydrofolate reductase (DHFR), only one, edatrexate, is an FPGS substrate. The other two, trimetrexate and piritrexim, are not capable of being glutamylated. Nonetheless, they possess potent, selective antineoplastic activity [7]. Such agents may be particularly useful for avoiding natural resistance [24, 32] and overcoming acquired resistance to antifolate chemotherapy [23].

This understanding has prompted the development of a new generation of nonpolyglutamatable antifolates. Some of these compounds resemble trimetrexate and piritrexim, since they lack a glutamyl sidechain. Such structures represent a major departure from classical antifolates like MTX. In our laboratory, a series of structure-activity studies have indicated that more moderate changes in the terminal γ-carbon region of the aminopterin (AMT) structure would be beneficial [35].

A promising outcome of this strategy has been the development of N^{α}-(4-amino-4-deoxypteroyl)-N^{δ}-hem-

iphthaloyl-L-ornithine, PT523, a potent aminopterin analogue in which the glutamyl moiety has been replaced by N^{δ}-hemiphthaloyl-L-ornithine [34, 38]. Retention of the A, B and C rings of AMT, and its α-carboxyl group, and the introduction of a phthalamide tail have afforded a water-soluble product that selectively penetrates tumor cells via the reduced folate carrier (RFC) and may utilize additional cellular transport mechanisms, as recent studies have indicated [30, 34, 42]. The phthalamide group also makes a substantial contribution to DHFR binding by interacting with three amino acid residues in the enzyme's binding site, Pro 26, Arg 28 and Phe 31 [13, 22]. In consequence, the K_i of PT523 as a competitive inhibitor of human DHFR-catalyzed reduction of dihydrofolate is 0.35 p*M*, 15-fold lower than that of MTX [3, 22].

The present study reflects our continuing interest in the pharmacologic and toxicologic properties of PT523 [22, 30, 34, 37, 38] and had the following specific aims: to analyze the plasma pharmacokinetics of PT523 and MTX in a murine tumor model; to compare the impact of PT523 and MTX on 5,10-methylenetetrahydrofolate (CH_2THF) levels of tumor and normal host tissues; to synthesize [C-ring-UL-^{14}C]N^{α}-(4-amino-4-deoxypteroyl)-N^{δ}-hemiphthaloyl-L-ornithine ([^{14}C]PT523); and to determine the time-dependent distribution of [^{14}C]PT523 in tumor and normal host tissues.

Materials and methods

Reagents and tissues

PT523 and N^{α}-(4-amino-4-deoxypteroyl)-L-ornithine (APA-orn) were synthesized as described previously [37]. N^{α}-(4-Amino-4-deoxy-7-hydroxypteroyl)-N^{δ}-hemiphthaloyl-L-ornithine (HOP) was prepared from PT523 and partially purified rabbit liver aldehyde oxidase as part of another study [43]. MTX was a gift from Lederle Laboratories, Pearl River, N.Y. These compounds were >97% pure by high-performance liquid chromatography (HPLC) and ultraviolet spectrophotometry. [6-^{3}H]-5-Fluorodeoxyuridine-5′-monophosphate (^{3}H-FdUMP) was obtained from Moravek Biochemicals, City of Industry, Calif., and its purity checked regularly by HPLC. Recombinant *Lactobacillus casei* thymidylate synthase (TS) was prepared and purified as described previously [31], using an *Escherichia coli* vector donated by Dr. Daniel Santi, University of California, San Francisco. The SCC VII tumor, a gift from Dr. Martin Brown, Stanford University, Palo Alto, Calif., is a squamous cell carcinoma line initially derived by Dr. Herman Suit at the Massachusetts General Hospital, Boston, Mass, from the spontaneous abdominal wall tumor of a C3H mouse.

Stability of PT523 in solution

Acetate solutions at pH 5.0, 6.0, 7.0, 8.0 and 9.0 were prepared by titration of 0.4 *M* sodium acetate and 0.4 *M* acetic acid. To 4.95-ml aliquots of each stock solution was added 0.05 ml of 5 mg · ml^{-1} disodium PT523. Samples at each pH value were monitored for 5 days. One set was kept in the dark at 4 °C, another in the dark at 22 °C and the third at 22 °C, under ordinary fluorescent lighting. A 0.05 mg · ml^{-1} solution of PT523 was prepared in distilled water and maintained at 22 °C and another in pH 7.0 sodium acetate-acetic acid solution at 37 °C, both protected from light. Each solution was assayed daily by HPLC on a C18 column, 5 mm diameter x 100 mm long, eluted with 6% v/v acetonitrile in 0.13 *M* ammonium acetate (AmAc), pH 6.8, at 1 ml · min^{-1}. The retention volume of PT523 was 13.3 ml (HPLC method 1).

Pharmacokinetics of PT523 and MTX in tumor-bearing mice

Injectable PT523 was prepared by dissolving the free acid in two equivalents of NaOH. MTX formulated for clinical use was dissolved in sterile water. A group of 11 C3H male mice received 2×10^6 SCC VII tumor cells subcutaneously (s.c.) over the right flank and were treated with intraperitoneal (i.p.) drug when the median diameter was 6 mm along the long axis. A saline-treated control was sacrificed at 60 min. The other mice were treated with 77 μmol · kg^{-1} PT523. One was sacrificed immediately, and the others at 5, 10, 15, 20, 40, 60, 80, 100 and 120 min. The procedure was repeated with 77 μmol · kg^{-1} MTX. Since we had not determined whether or not PT523 pharmacokinetics were linear (AUC proportional to dose), equimolar doses were chosen for direct comparison of exposure and clearance. The blood was collected by cardiac puncture into heparinized syringes and centrifuged at 5500 *g* for 15 min at 4 °C. For analysis of ultrafiltrable PT523 or MTX, approximately 350 μl of each plasma sample was deproteinated through a Millipore Centrifree ultrafilter. For analysis of total PT523 and MTX, samples and standards were treated with two volumes of absolute methanol, centrifuged at 16 000 *g* for 20 min and the supernatants collected. An internal standard, *N*,*N*-dimethylaminobenzoic acid (DABA) was added to a final concentration of 5 μ*M*. Samples and standards were analyzed by HPLC on a 5-mm diameter × 100-mm long C18 column with 7% v/v acetonitrile in 0.1 *N* AmAc, pH 6.0, at a flow rate of 2.3 ml · min^{-1} (HPLC method 2). Retention volumes for PT523, MTX and DABA were 30.6, 33.3 and 43.2 ml, respectively. Five replicates were performed.

Standard pharmacokinetic parameters, area under the concentration (C) vs time (t) curve (AUC, μM · min), area under the C × t vs t curve (AUMC, μM · min^2), whole body clearance (Cl_t, ml · min^{-1}), steady-state volume of distribution (V_{ap}, ml·kg^{-1}) and mean residence time (MRT, min) were calculated by noncompartmental analysis [20].

CH_2THF pool size

Tumor, intestinal mucosa, and marrow from the long bones were harvested from the mice used for the pharmacokinetic experiments, kept at 4 °C, treated with 0.8% ammonium chloride, washed with phosphate-buffered saline, extracted as previously described, and assayed for total CH_2THF content by the method of Priest and Doig [33, 44]. Protein content (in milligrams) was determined by the Bradford dye-binding method [10]. Samples were frozen at –75 °C between assays. Five replicates were performed on different days.

Preparation of [^{14}C]PT523

An 88.5 mg, 192 μmol portion of APA-orn was finely pulverized in 5 ml *N*,*N*-dimethylformamide (DMF) by 45 min of sonication in an ultrasonic cleaning bath. The suspension was kept at 20 °C and 166 μmol [ring UL-^{14}C]phthalic anhydride (5 mCi) was added. The suspension dissolved rapidly. After 3 days at 22 °C, the DMF was evaporated. The residue was purified in four equal batches by preparative HPLC on a 25 mm × 100 mm Prep Pak C18 column. The eluent was 0.01 *M* AmAc, pH 7.7, with a 45-min linear acetonitrile gradient from 5% to 12% v/v. The flow rate was 10 ml · min^{-1}. The product was collected in the 200—275-ml fraction and analyzed by HPLC or a 5 mm dia × 100 mm long C18 column. The AmAc pH was 4.0 and a 90-min linear acetonitrile gradient from 0% to 20% was used with a 1 ml · min^{-1} flow rate (HPLC method 3). Fractions of 0.5 ml each were also analyzed by liquid scintillation counting (LSC). Nonradioactive standards had the following approximate retention volumes: phthalic acid, 9 min; HOP, 23 min; and PT523, 33 min.

Tissue distribution of [^{14}C]PT523 in a murine tumor model

Five male C3H mice weighing 30 ± 4 g received 2×10^6 SCC VII tumor cells s.c. in the right flank. Tumor diameters were determined daily by two-dimensional caliper measurements [5]. When the median for the group reached 6 mm along the long axis, 15 μmol · kg^{-1} [^{14}C]PT523, specific activity 10 000 dpm · nmol^{-1}, was injected through the tail vein.

The mice were placed in metabolic cages. At 0.25, 1 or 6 h after injection, a mouse was removed and sacrificed by cervical dislocation. At 24 h, two mice were used. The visceral membranes and rib cages were opened with dissecting scissors, taking care to avoid nicking any organs. Blood was collected from the vena cava into a 1-ml heparinized syringe with a 23 gauge needle.

The blood samples were centrifuged at 5500 *g* for 15 min at 4 °C, pellets collected, washed with phosphate-buffered saline, and stored at –80 °C. The bladder urine was collected, pooled with the cage urine, weighed and frozen at –80 °C. The long bones, kidneys, liver, spleen, heart, lungs, pancreas, testicles, brain, flank muscles, small intestine, colon and tumor were excised and the feces were collected. The marrow was harvested by forcing 500 μl of phosphate-buffered saline through the shafts of the long bones with 23 gauge needles. The small intestine and colon were opened lengthwise for removal of the contents, washed with ice-cold phosphate-buffered saline, weighed, frozen in glass vials on dry ice and stored at –80 °C.

The frozen samples were homogenized at 4 °C with the aid of 1.0 ml distilled water in a Branson biohomogenizer. Except for one of the additional mice treated with PT523 for 24 h, plasma, urine, homogenized organs, blood cells and feces were digested for 24 h at room temperature with 0.1 volume of 10 *N* NaOH, neutralized with 1 *N* acetic acid and analyzed by LSC. Quench determinations were performed for each sample. For analysis of possible metabolites, homogenized samples from a second mouse sacrificed at 24 h were mixed with 3 volumes of methanol and centrifuged at 23 000 *g* for 20 min. The supernatants were evaporated under nitrogen at 45 °C, and analyzed by HPLC method 3. Three replicates were performed.

Results

After 5 days in the dark, PT523 solutions kept between pH 5 and pH 9 showed < 1% decomposition at 4 °C, but at 22 °C, the pH 5 solution decomposed with a half-life of 2.9 days. At 37 °C, the half-life of the pH 7 solution was 70 days. Solutions of disodium PT523 were stable for ≥5 days at pH 8 and 22 °C in the dark. After 1 day under fluorescent lighting, the pH 8 samples were 50%, pH 9 samples 93%, and pH 5–7 samples 100% decomposed.

Figure 1 shows C vs t plots for 77 μmol · kg^{-1} MTX and PT523. Peak times (t_{max}) of total MTX and PT523, were 10 and 15 min. Corresponding peak concentrations (C_{max}) were 306 and 115 μ*M*. The respective AUC (μM · min), MRT (min), Cl_t, (ml · min^{-1}), and V_{ap}, (ml · kg^{-1}) of total MTX (mean ± standard deviation, $n = 5$) were 6472 ± 91, 16 ± 3.2, 0.36 ± 0.005, and 325 ± 110; and those of total PT523 were 4311 ± 604, 20 ± 3.6, 0.56 ± 0.08 and 532 ± 103. MTX was 30% and PT523 was 70% reversibly bound to plasma macromolecules.

Within 20 min of administration of PT523, tumor CH_2THF fell from 1.4 to 0.2 nmol · mg^{-1} protein and remained low for ≥240 min. With MTX, the same 20 min nadir was seen, but from 80 min after injection,

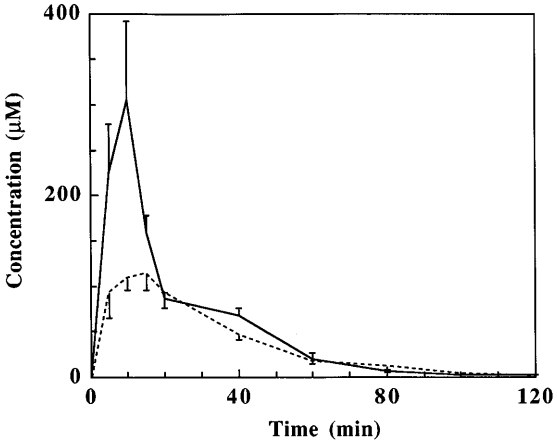

Fig. 1 Plot of plasma concentration versus time after administration of 77 μmol · kg^{-1} MTX (*solid line*) or PT523 (*dashed line*). Semi-bars one-half the standard error of the mean of five determinations

CH_2THF pools gradually rebounded. By 240 min after injection, mean levels had reached 1.1 nmol · mg^{-1} protein (Fig. 2). Cytosolic pools of CH_2THF in the gut and marrow were also monitored (Fig. 3). Within 5 min of PT523 injection, CH_2THF levels in the gut had dropped from 0.9 to 0.1 nmol · mg^{-1} protein, where they remained for approximately 90 min. By 240 min, levels had recovered to 0.4 nmol · mg^{-1} protein. With MTX, 20 min was required to reach a nadir of 0.2 nmol · mg^{-1} protein. Recovery after PT523 administration resembled that after MTX administration. Marrow levels of CH_2THF were not substantially altered by PT523 or MTX.

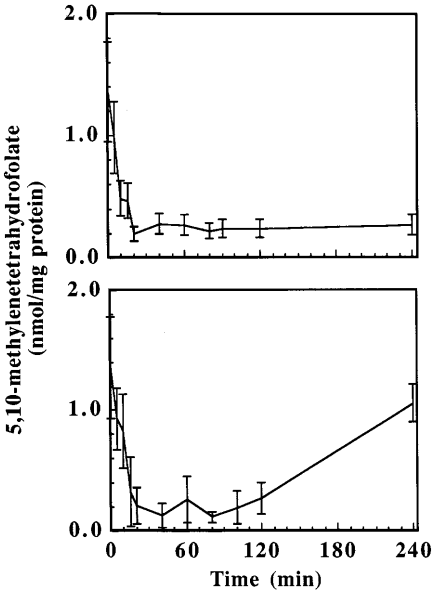

Fig. 2 Plots of SCC VII tumor cytosolic pools of CH_2THF versus time after i.p. bolus administration of 77 μmol · kg^{-1} PT523 (*above*) or MTX (*below*). *Bars* standard error of the mean of five determinations

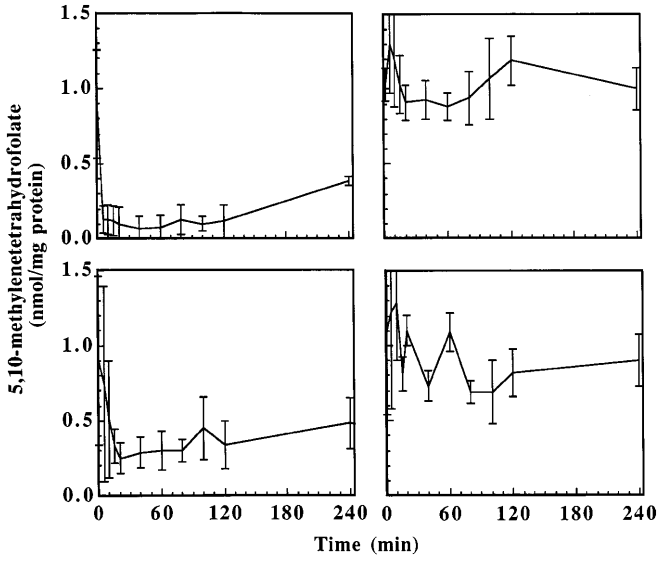

Fig. 3 Plots of small intestinal mucosal (*left*) and bone marrow (*right*) cytosolic pools of CH_2THF versus time after administration of 77 μmol · kg^{-1} PT523 (*above*) or MTX (*below*). *Bars* standard error of the mean of five determinations

From the synthesis of [^{14}C]PT523, Fig. 4, 80 μmol were obtained, a 46% yield, based on [^{14}C]phthalic acid, specific activity 30 Ci · mol^{-1}, radiochemical purity 95%. The tissue distribution of [^{14}C]PT523 is shown in Fig. 5 and 6. Maximum uptake into kidney and duodenum came 1 h after injection, in colon after 6 h, and in other organs, tumor, and packed blood and marrow cells within 15 min. After 15 min, 26% of the dose was in the liver, 6% in the tumor, other organs, marrow and packed blood cells, 2% in the urine, none in the feces, and 66% was unrecovered. At 1 h, 15% was in the washed small intestine, 8% in the liver, 8% in the urine, 2% in the kidneys and 2% in the tumor, other organs, marrow and blood cells; fecal ^{14}C was miniscule, and 65% was unrecovered. At 6 h, 18% was in the feces, 13% in the urine, 1% in the organs, tumor, marrow and blood cells, and 68% was unrecovered. At 24 h, 26% of the dose was in the feces, 9% in the urine, $<1\%$ in the

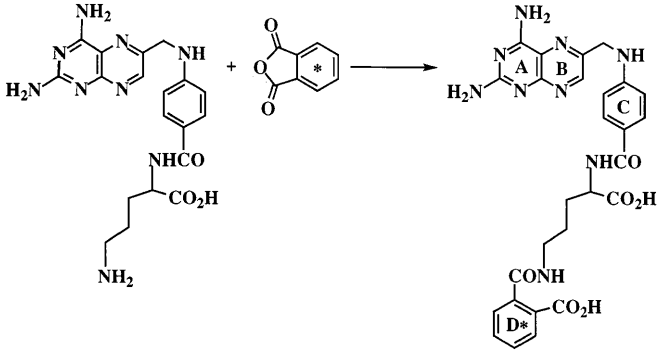

Fig. 4 Reaction schematic for the synthesis of [^{14}C]PT523 from APA-orn and [ring UL-^{14}C]phthalic anhydride. The asterisk indicates general labeling of the six ring carbons with ^{14}C

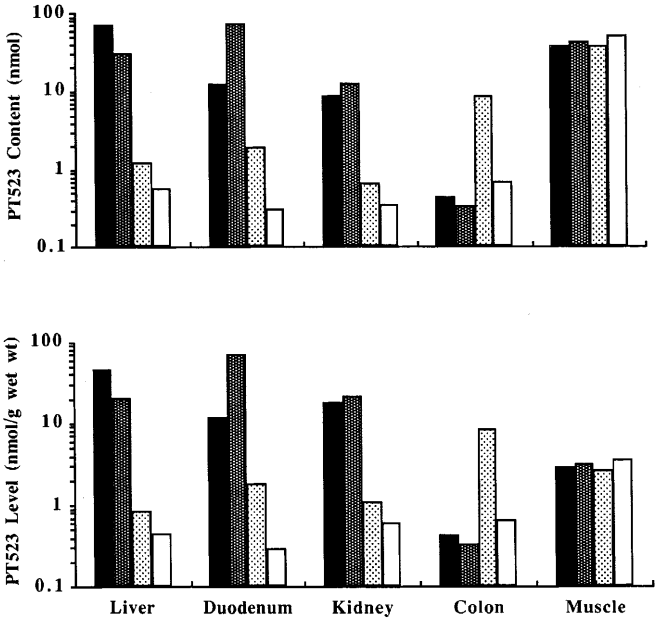

Fig. 5 Content (nanomoles, *upper panel*) and level (nanomoles per gram wet weight, *lower panel*) of ^{14}C in C3H mouse tissues identified as determinants of MTX disposition [8] at 0.25 (*black*), 1.0 (*dark gray*), 6.0 (*light gray*) and 24 h (*white*) after i.v. administration of a 15 μmol · kg^{-1} bolus of [^{14}C]PT523

organs, tumor, marrow and blood cells, and 64% was unrecovered.

No measurable [^{14}C]phthalic acid or [^{14}C]HOP was found in feces, blood cells or organ extracts 24 h after PT523 treatment. Of the total injected ^{14}C, $>95\%$ was [^{14}C]PT523, indicating no significant cleavage of the phthaloyl group or other metabolism. Minor changes in composition were seen in tumor, liver and urine chromatograms (Fig. 7). In the tumor extract, $>92\%$ of the total counts per minute were [^{14}C]PT523. Five small, unidentified peaks also appeared. The liver extract contained 12% of its ^{14}C as HOP, the only detected metabolite. Two peaks from the 24-h urine had the same retention volumes as HOP and phthalic acid. They comprised, respectively, 5% and 9% of the total urinary ^{14}C. Three small, unidentified radioactive peaks also appeared in the chromatogram.

Discussion

Stability tests showed that a sterile water solution of disodium PT523 in an amber bottle was the appropriate parenteral dosage form.

Comparison of t_{max} values showed that absorption of PT523 from the peritoneal cavity was slower than that of MTX. The rate of MTX transport from the peritoneal space to the circulation is proportional to the permeability-area product (PA, ml · min^{-1}) of the peritoneal membrane [11]. For water-soluble drugs, PA is inversely proportional to the square-root of molecular weight [17]. The reported value for MTX was 8 ml · min^{-1}; hence

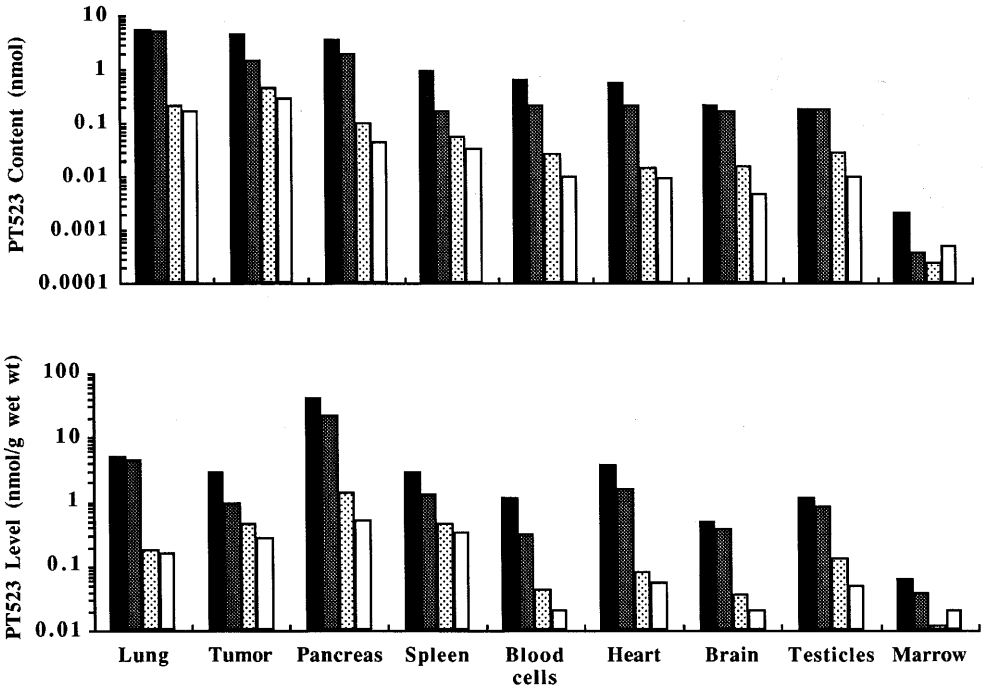

Fig. 6 Content (nanomoles, *upper panel*) and level (nanomoles per gram wet weight, *lower panel*) of ^{14}C in SCC VII tumor and C3H mouse tissues identified as determinants of MTX antifolate activity [43] at 0.25 (*black*), 1.0 (*dark gray*), 6.0 (*light gray*) and 24 h (*white*) after i.v. administration of a 15 μmol · kg^{-1} bolus of [^{14}C]PT523

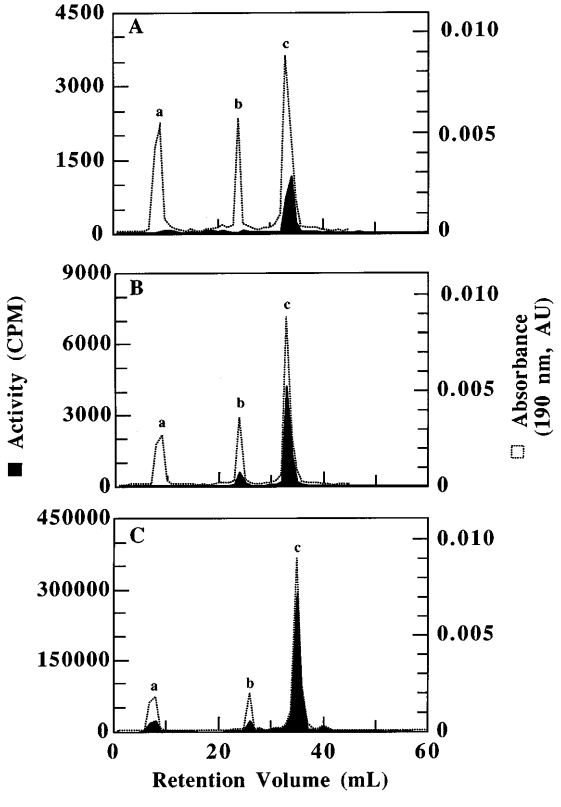

Fig. 7A–C Radiochromatograms of (**A**) tumor cytosol, (**B**) liver cytosol, and (**C**) urine collected 24 h after i.v. administration of a 15 μmol · kg^{-1} bolus of [^{14}C]PT523. *Black peaks* cpm of [^{14}C], *dotted peaks* A_{190} of nonradioactive standards for (*a*) phthalic acid, (*b*) 7-hydroxy-PT523, and (*c*) PT523

that of PT523 is 7 ml · min^{-1}. Pharmacokinetic analysis showed that the AUC of PT523 was 33% less than that of MTX, owing to its more rapid Cl_t. Bischoff et al. have found that MTX is 25% protein-bound in their mouse model [8]. In ours, MTX was 30% reversibly bound to plasma proteins and a proportion was incorporated into cells and tissues. A greater fraction of PT523, 70%, was reversibly bound to plasma proteins, yet its V_{ap} (532 ml · kg^{-1}) was greater than that of MTX (7.2 times the blood volume). The V_{ap} of MTX (325 ml · kg^{-1}) was 4.4 times the blood volume (51 ml·kg^{-1}), but only 42% of total body water (766 ml · kg^{-1}), for a 30-day-old mouse. When V_{ap} is 100–400 ml · kg^{-1}, $t_{1/2}$ is a function of tissue binding only [6]. From these data we conclude that more PT523 than MTX partitioned into extravascular cells and tissues [19].

CH_2THF levels, monitored for 4 h after MTX or PT523 administration, showed a decline in tumor to 10% of baseline within 20 min. At 4 h after MTX treatment the CH_2THF pool returned to 85% of the baseline value, but with PT523 there was no recovery. The more persistent antifolate effect of PT523 is consistent with its ability to inhibit the growth of SCC VII cells in vivo [38].

Although MTX polyglutamates may target other folate-metabolizing enzymes [1, 2], the principal target of MTX and PT523 is DHFR [29]. In mice, mucositis is the dose-limiting toxicity of MTX [26]. CH_2THF depletion of gut mucosa by PT523 may be more severe and rapid (90% inhibition within 5 min) than that of equimolar MTX (70% inhibition within 20 min). After 4 h, similar recovery is seen with both drugs. In bone marrow, neither drug appears to decrease CH_2THF levels significantly.

[^{14}C]PT523 was synthesized for use as a tissue distribution tracer by acylation of APA-orn with [^{14}C]phthalic anhydride. Within 15 min of its i.v. administration to tumor-bearing mice, the largest amount of [^{14}C]PT523 was in the liver. After 1 h, the liver content decreased slightly, but that of the duodenum rose abruptly, and 5 h later the colon level increased. Similar patterns have been reported for MTX in tumor- and non-tumor-bearing mice [9, 41, 45].

In an earlier study, Bischoff et al. cannulated the bile ducts of mice prior to i.v. administration of MTX and found bile concentrations 300-fold greater than plasma levels. Biliary excretion resulted in peak gut levels 1 h after injection. Owing in part to enterohepatic recirculation [8], MTX recovery from urine exceeded that from feces. Recent work has shown that MTX is excreted into bile via the cMOAT transporter [27], which has been cloned and characterized [39]. We did not analyze PT523 in bile, but the high gut levels at 1 h are consistent with biliary excretion. We also detected maximum colon levels of PT523 at 6 h, and found substantial amounts in the feces. Henderson et al. administered 33 $\mu mol \cdot kg^{-1}$ MTX and 24 h afterward found 55% of the dose in the urine and 40% in the feces. The urine/feces ratio was dose dependent: 24 h after a 1.1 $\mu mol \cdot kg^{-1}$ dose, 79% was in the urine versus 10% in the feces [21]. In the present study with 15 $\mu mol \cdot kg^{-1}$ PT523, only 9% was in the urine versus 26% in the feces at 24 h. Apparently less PT523 is enterohepatically recirculated.

As shown in Figs. 5 and 6, more elevated levels ($nmol^{-1} \cdot g$ wet weight of $tissue^{-1}$) and content (nmol) of PT523 were found in the liver, gut, kidney, lung and pancreas at all time-points. The high PT523 content of gut and tumor, but not of bone marrow, are consistent with the changes in their respective CH_2THF pools (Figs. 2 and 3). Similar patterns have been reported by Zaharko et al. for incorporation of ^{3}H from ^{3}H-deoxyuridine and ^{3}H-deoxythymidine into DNA during and after 48 h of continuous MTX infusion into mice [46].

An additional cytotoxicity mechanism is possible for PT523 if the hemiphthaloyl group is removed by metabolism or chemical decomposition within cells. The product, APA-orn, is an inhibitor of FPGS [12]. Radiochromatograms of tissue extracts revealed traces of phthalic acid, but only in the urine (Fig. 7). Extracellular APA-orn did not appear to penetrate tumor or host tissues, in agreement with our earlier studies with cell lines in tissue culture [36].

In summary, clearance of PT523 was 50% more rapid and plasma protein binding 2.3-fold greater than that of MTX. Its greater volume of distribution and diminished excretion showed that PT523 partitioned more extensively than MTX into extravascular tissues. PT523 elimination was consistent with substantial biliary secretion, but less enterohepatic resorption than with MTX. In its antifolate effect, PT523 targeted SCC VII tumor and, less persistently, gut but selectively spared bone marrow. PT523 distributed predominantly into the larger organs with a better blood supply: liver, gut, and kidneys.

References

1. Allegra CJ, Chabner BA, Drake JC, Lutz R, Rodbard D, Jolivet J (1985) Enhanced inhibition of thymidylate synthase by methotrexate polyglutamates. J Biol Chem 260: 9720
2. Allegra CJ, Drake, Jolivet J, Chabner BA (1985) Inhibition of phosphoribosyl aminoimidazolecarboxamide formyltransferase by methotrexate and dihydrofolic acid polyglutamates. Proc Natl Acad Sci USA 82: 4881
3. Appleman JR, Prendergast N, Delcamp TJ, Freisheim JH, Blakley RL (1988) Kinetics of the formation and isomerization of methotrexate complexes of recombinant human dihydrofolate reductase. J Biol Chem 263: 10304
4. Barredo J, Moran RG (1992) Determinants of antifolate cytotoxicity: folylpolyglutamate synthetase activity during cellular proliferation and development. Mol Pharmacol 42: 687
5. Begg AC (1987) Principles and practices of the tumor growth delay assay. In: Kalman RF (ed) Rodent tumor models. Pergamon Press, New York, pp 114–121
6. Benowitz N, Forsyth RP, Melmon KL, Rowland M (1974) Lidocaine disposition kinetics in monkey and man: I. prediction by a perfusion model. Clin Pharmacol Ther 16: 87
7. Bertino JR, Kamen B, Romanini A (1997) Folate antagonists. In: Holland JF, Bast RC Jr, Morton DL, Frei E III, Kufe DW, Weichselbaum RR (eds) Cancer medicine, 4th edn. Williams & Wilkins, Baltimore, p 907
8. Bischoff KB, Dedrick RL, Zaharko DS (1970) Preliminary model for methotrexate pharmacokinetics. J Pharm Sci 59:149
9. Bischoff KB, Dedrick RL, Zaharko, Longstreth JA (1971) Methotrexate pharmacokinetics. J Pharm Sci 60: 1128
10. Bradford MM (1976) A rapid and sensitive method for the quantitation of microgram quantities of protein utilizing the principle of protein-dye binding. Anal Biochem 72: 248
11. Chen H-S G, Gross JF (1979) Physiologically based pharmacokinetic models for anticancer drugs. Cancer Chemother Pharmacol 2: 85
12. Clarke L, Rosowsky A, Waxman DJ (1986) Inhibition of human liver folatepolyglutamate synthetase by non-γ-glutamatable antifolate analogs. Mol Pharmacol 31: 122
13. Cody V, Galitsky N, Luft JR, Pangborn W, Rosowsky A, Blakley RL (1997) Comparison of two independent crystal structures of human dihydrofolate reductase ternary complexes with NADPH and the very tight binding inhibitor PT523. Biochem 36: 13897
14. Cowan KH, Jolivet JA (1984) A methotrexate-resistant human breast-cancer cell line with multiple defects including diminished formation of methotrexate polyglutamates. J Biol Chem 259: 10793
15. Curt GA, Jolivet J, Bailey BD (1984) Synthesis and retention of methotrexate polyglutamates by human small cell lung cancer. Biochem Pharmacol 33: 1682
16. Curt GA, Jolivet J, Carney DN, Bailey BD, Drake JC, Clendeninn NJ, Chabner BA (1985) Determinants of the sensitivity of human small-cell lung cancer cell lines to methotrexate. J Clin Invest 76: 1323
17. Dedrick RL, Myers CE, Bungay PM, DeVita VT, Jr (1978) Pharmacokinetic rationale for peritoneal drug administration in the treatment of ovarian cancer. Cancer Treat Rep 62: 1
18. Fabre I, Fabre G, Goldman ID (1984) Polyglutamylation, an important element in methotrexate cytotoxicity and selectivity in tumor versus murine granulocytic progenitor cells. Cancer Res 44: 3190
19. Gibaldi M, Perrier D (1982) Pharmacokinetics, 2nd edn. Marcel Dekker, New York, p 210
20. Gibaldi M, Perrier D (1982) Pharmacokinetics, 2nd edn. Marcel Dekker, New York, pp 409–417

21. Henderson ES, Adamson RH, Denham C, Oliverio VT (1965) The metabolic fate of tritiated methotrexate I. Absorption, excretion and distribution in mice, rats, dogs and monkeys. Cancer Res 25: 1008
22. Johnson JM, Meiering EM, Wright JE, Pardo J, Rosowsky A, Wagner G (1997) NMR solution structure of the antitumor compound PT523 and NADPH in the ternary complex with human dihydrofolate reductase. Biochemistry 36: 4399
23. Li W-W, Bertino JR (1992) Inability of leucovorin to rescue a naturally methotrexate-resistant human soft tissue sarcoma cell line from trimetrexate cytotoxicity. Cancer Res 52: 6886
24. Li W-W, Lin JT, Schweitzer BI, Bertino JR (1991) Mechanisms of sensitivity and natural resistance to antifolates in a methylcholanthrene-induced rat sarcoma. Mol Pharmacol 40: 854
25. Li WW, Waltham M, Tong W, Schweitzer BI, Bertino JR (1993) Increased activity of γ-glutamyl hydrolase in human sarcoma cell lines: a novel mechanism of intrinsic resistance to methotrexate. In: Ayling JE, Nair MG, Baugh CM (eds) Chemistry and biology of pteridines and folates. Plenum Press, New York, p 635
26. Margolis S, Phillips FS, Sternberg SS (1971) The cytotoxicity of methotrexate in mouse small intestine in relation to inhibition of folic acid reductase and of DNA synthesis. Cancer Res 31: 2037
27. Masayuki M, I'izuka Y, Yamazaki M, Nishigaki R, Kato Y, Ni'inuma K, Suzuki H, Sigiyama Y (1997) Methotrexate is excreted into the bile by canalicular multispecific organic anion transporter in rats. Cancer Res 57: 3506
28. McGuire JJ, Mini E, Hsieh P, Bertino JR (1985) Role of methotrexate polyglutamates in methotrexate- and sequential methotrexate-5-fluorouracil-mediated cell kill. Cancer Res 45: 6395
29. Osborne MJ, Freeman M, Huennekens FM (1958) Inihibition of dihydrofolic reductase by aminopterin and amethopterin. Proc Soc Exp Biol Med 97: 429
30. Peters GJ, Braakhuis BJM, Rosowsky A, Kegel A, Rots M, van der Wilt CL, Pinedo HM, Jansen G (1997) Preclinical activity of PT523 in relation to transport. Pteridines 8: 118
31. Pinter K, Davisson VJ, Santi DV (1988) Cloning, sequencing and expression of the *Lactobacillus casei* thymidylate synthase gene. DNA 7: 235
32. Pizzorno G, Chang Y-M, McGuire JJ, Bertino JR (1989) Inherent resistance of human squamous carcinoma cell lines to methotrexate as a result of decreased polyglutamylation of this drug. Cancer Res 49: 5275
33. Priest DG, Doig MT (1986) Tissue folate polyglutamate chain-length determination by electrophoresis as thymidylate synthase-fluorodeoxyuridylate complexes. In: McCormick DB, Chytill F (eds) Methods in enzymology, vol 122. Academic Press, New York, pp 313–319
34. Rhee MS, Galivan J, Wright J, Rosowsky A (1994) Biochemical studies of PT523, a potent nonpolyglutamatable antifolate, in cultured cells. Mol Pharmacol 45: 783
35. Rosowsky A (1989) Chemistry and biological activity of antifolates. In: Ellis GP, West GB (eds) Progress in medicinal chemistry. Elsevier Science Publishers, New York, pp 158–226
36. Rosowsky A, Freisheim JH, Moran RG, Solan V, Bader H, Wright JE, Radike-Smith M (1986) Methotrexate analogues. 26. Inhibition of dihydrofolate reductase and folylpolyglutamate synthase activity and in vitro tumor cell growth by methotrexate and aminopterin analogues containing a basic amino acid side chain. J Med Chem 29: 655
37. Rosowsky A, Bader H, Forsch RA (1989) Synthesis of the folylpolyglutamate sythetase inhibitor N^{α}-pteroyl-L-ornithine and its N^{δ}-benzoyl and N^{δ}-hemiphthaloyl derivatives, and an improved synthesis of N^{α}-(4-amino-4-deoxypteroyl)-N^{δ}-hemiphthaloyl-L-ornithine. Pteridines 1: 91
38. Rosowsky A, Vaidya C, Bader H, Wright J, Teicher BA (1997) Analogues of N^{α}-(4-amino-4-deoxypteroyl)-N^{δ}-hemiphthaloyl-L-ornithine (PT523) modified in the side chain: Synthesis and biological evaluation. J Med Chem 40: 286
39. Saito H, Masuda S, Inui K (1997) Cloning and functional characterization of a novel rat organic anion transporter mediating basolateral uptake of methotrexate in the kidney. J Biol Chem 271: 20719
40. Schlemmer SR, Sirotnak FM (1993) Retentiveness of methotrexate polyglutamates in cultured L1210 cells. Evidence against a role for mediated plasma membrane transport outward. Biochem Pharmacol 45: 1261
41. Uadia P, Blair AH, Ghose T (1984) Tumor and tissue distribution of a methotrexate-anti-EL4 immunoglobulin conjugate in EL4 lymphoma bearing mice. Cancer Res 44: 4263
42. Westerhof GR, Schornagel JH, Kathmann I, Jackman AL, Rosowsky A, Forsch RA, Hynes JB, Boyle FT, Peters GJ, Pinedo HM, Jansen G (1995) Carrier- and receptor-mediated transport of folate antagonists targeting folate dependent enzymes: Correlates of molecular-structure and biological activity. Mol Pharmacol 48: 459
43. Wright JE, Rosowsky A, Waxman DJ, Trites D, Cucchi CA, Flatow J, Frei E III (1987) Metabolism of methotrexate and γ-*tert*-butyl methotrexate by human leukemic cells in culture and by hepatic aldehyde oxidase *in vitro*. Biochem Pharmacol 36: 2209
44. Wright JE, Dreyfuss A, El-Magharbel I, Trites D, Jones SM, Holden SA, Rosowsky A, Frei E III (1989) Selective expansion of 5,10-methylenetetrahydrofolate pools and modulation of 5-fluorouracil antitumor activity by leucovorin, *in vivo*. Cancer Res 49: 2592
45. Yang KH, Fung WP, Lutz RJ, Dedrick RL, Zaharko DS (1979) *In vivo* methotrexate transport in murine Lewis lung tumor. J Pharm Sci 68: 941
46. Zaharko DS, Fung W-P, Yang K-H (1977) Relative biochemical aspects of low and high doses of methotrexate in mice. Cancer Res 37: 1602